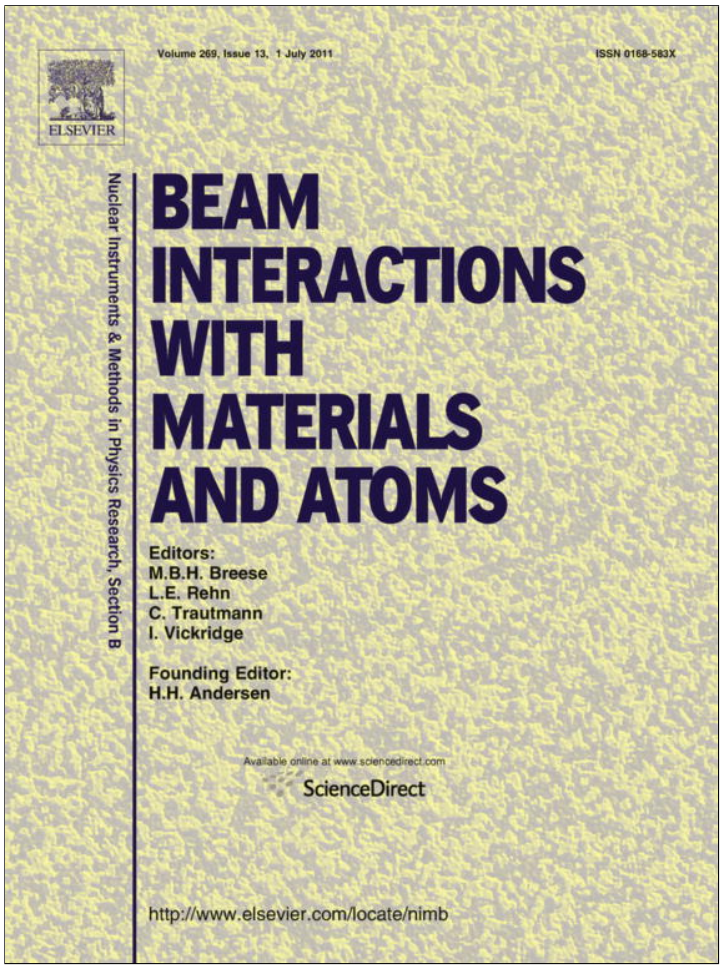

Nuclear Instruments and Methods in Physics Research B 269 (2011) 1527–1533

Contents lists available at ScienceDirect

Nuclear Instruments and Methods in Physics Research B

journal homepage: www.elsevier.com/locate/nimb

# Efficient two-step Positronium laser excitation to Rydberg levels

S. Cialdi [a,b], I. Boscolo [a,b], F. Castelli [a,b], F. Villa [a,b,*], G. Ferrari [c,d,e], M.G. Giammarchi [b]

[a] Università degli Studi di Milano, via Celoria 16, 20133 Milano, Italy
[b] Istituto Nazionale di Fisica Nucleare, sezione di Milano, via Celoria 16, 20133 Milano, Italy
[c] INO-CNR BEC Center, via Sommarive 14, 38123 Povo, Trento, Italy
[d] LENS-Università di Firenze, via Carrara 1, 50019 Sesto Fiorentino, Italy
[e] Istituto Nazionale di Fisica Nucleare, Gruppo collegato di Trento, via Sommarive 14, 38123 Povo, Trento, Italy

ARTICLE INFO

*Article history:*
Received 31 March 2010
Received in revised form 7 April 2011
Available online 23 April 2011

*Keywords:*
Positronium
Rydberg states
Zeeman and Stark effects

ABSTRACT

Antihydrogen production by charge exchange reaction between Positronium atoms and antiprotons requires efficient excitation of Positronium atoms up to high-$n$ levels (Rydberg levels). A two-step optical excitation, the first from ground to $n = 3$ and the second from this level to a Rydberg level, is proposed and a suitable laser system is discussed. The requirements on the energy and bandwidth of the excitation laser suggest the use of optical parametric generation technology for both wavelengths. The laser system is composed by two subsystems: one for the generation of 205 nm radiation and the other for the generation of 1670 nm radiation. We have separately developed and tested the laser sources and results are here presented.



## 1. Introduction

Efficient Positronium (Ps) excitation to high-$n$ levels is pursued in some experiments on antihydrogen $\overline{H}$ generation. In the AEGIS (Antimatter Experiment: Gravity, Interferometry, Spectroscopy) experiment [1–3] the production of cold $\overline{H}$ bunches in highly excited states (Rydberg states) would occur in the charge transfer of a cloud of Rydberg excited Ps atoms with a bunch of cold antiproton $\bar{p}$ by means of the reaction $Ps^* + \bar{p} \rightarrow \overline{H}^* + e^-$ [4–6].

The number of antihydrogen atoms produced is proportional to the cross-section of the charge exchange reaction, which is a function of the fourth power of the principal quantum number $n$ of the excited Ps [4–6] ($\sigma \propto n^4 \pi a_0^2$, where $a_0$ is the Bohr radius). Choosing $n$ in the range from 20 to 30, as in AEGIS proposal, increases substantially the recombination efficiency; a larger value of $n$ must be avoided because of ionization losses in the AEGIS environment [7].

Positronium excitation to these high-$n$ levels can be obtained either via collisions or via photon excitation. In the ATRAP experiment [4–6] Rydberg Ps generation was proposed and tested through the exchange reaction between laser excited Cs atoms and positrons. Cesium atoms and positrons drift almost continuously into a reaction chamber, and the production of antihydrogen was essentially a continuous process. In the AEGIS experiment the scheme has to meet the request of excited Ps in short timed dense bunches, for time of flight measurements on the produced antihydrogen atoms. Therefore, in our proposal positron bunches (20 nm long) are created and implanted in a converter providing Ps bunches. These atoms are directly excited to Rydberg levels by two simultaneous nanosecond laser pulses with different wavelengths [1]. The theory of pulsed Ps photon excitation in AEGIS is presented in Ref. [7].

In particular, Ps atoms are efficiently produced at a porous silica surface by hitting the silica sheet with a positron bunch at kinetic energies ranging from several 100 eV to a few kilo-electron volt [8–10]. Ps atoms leaving the target surface form an expanding cloud with an initial transverse area of the order of 1 mm diameter, at an effective temperature of the order of 100 K which corresponds to a velocity $v \sim 3 \times 10^4$ m/s RMS. The atoms move in a relatively strong magnetic field $\vec{B}$ of about 1 T [1]. In these conditions the combination of the Doppler, motional Stark, linear and quadratic Zeeman effects [7,11,12] results in a broadening of the excitation transition frequencies of the order of 1 THz, making the excitation process substantially less selective than in the usual case of Rydberg spectroscopy. This is one of the challenges that the laser system in AEGIS has to face. The characteristics of laser pulses in terms of power and spectral bandwidth must be tailored to the geometry, the level-bandwidths and the timing of the Ps expanding cloud in order to maximize the excitation efficiency of the whole Ps cloud within few nanoseconds.

The photo-excitation of Ps to high-$n$ state requires photon wavelengths close to 182 nm (6.8 eV). The generation of such a laser wavelength, with a definite frequency band and a well defined power and timing, constitutes a difficult task. Moreover, a certain

* Corresponding author at: Università degli Studi di Milano, via Celoria 16, 20133 Milano, Italy. Tel.: +39 0250317633.
*E-mail address:* fabio.villa@unimi.it (F. Villa).

0168-583X/$ - see front matter © 2011 Elsevier B.V. All rights reserved.
doi:10.1016/j.nimb.2011.04.108

flexibility in the laser operation is required being the experiment characteristics not-completely closed. UV market lasers providing that frequency do not seem to comply to the requirements of AEGIS experiment, at the authors' knowledge. Therefore we have considered excitation via a two-step optical transition, by exploiting two possible alternatives: the path composed by the transitions $1 \rightarrow 2$ and $2 \rightarrow$ high-$n$, and the path with the transitions $1 \rightarrow 3$ and $3 \rightarrow$ high-$n$. Even if the $1 \rightarrow 2$ transition is well known [13,14] and the two photon excitation via $1 \rightarrow 2 \rightarrow$ high-$n$ was tested in [15], we have selected the $1 \rightarrow 3 \rightarrow$ high-$n$ excitation path for the following considerations [7,18]: (i) the level $n = 2$ has a lifetime of 3 ns, shorter than the 10.5 ns of the level $n = 3$; (ii) the excitation efficiency, calculated in [7] by referring to the saturation fluence defined later, results greater in the $1 \rightarrow 3 \rightarrow$ high-$n$ transitions; (iii) the total laser energies per pulse, required to reach saturation fluencies, are definitely lower in the second sequence than in the first one [18]. The longer lifetime is less demanding about the time-jitter between the two laser pulses and the higher excitation efficiency allows to have more antihydrogen atoms after charge exchange reaction. Finally, lower laser energies are useful in order to maintain easily the low temperature of the cryogenic environment.

Our laser system is based on a Q-switched Nd:YAG producing $\sim 5$ ns pulses used to pump nonlinear crystals for parametric generation of the desired wavelengths having a broad, continuum spectrum in order to efficiently cover the Ps Rydberg band, as discussed in the following section. With this scheme we perform a two step incoherent excitation to Rydberg levels and an efficiency up to 30% is expected [7], slightly lower than the theoretical efficiency of 33% attainable discarding spontaneous emission and ionization. Other excitation systems can be envisaged in order to obtain better population transfer efficiencies, like $\pi$ coherent pulses or adiabatic passage techniques [16,17]. These schemes require carefully prepared transform limited and/or chirped laser pulses. Because Ps excitation in our experiment needs laser pulses with a very broad linewidth and a time duration not longer than few nanoseconds, as required by the constraints of exciting the population more rapidly than Ps ground state decay by annihilation and Ps ballistic expansion timing, these schemes can be of complicate, difficult and expensive implementation. Our proposal has the advantage of a more simple and cost-effective realization.

## 2. Ps excitation from $n = 1$ to high-$n$ levels

The detailed theory of Ps excitation to Rydberg states is presented in Refs. [7,18]; here we report the results relevant to the laser system discussion. The Ps excitation is performed by a two step transition: a resonant one from $n = 1$ to $n = 3$ and a near resonant one from $n = 3$ to high-$n$. The $1 \rightarrow 3$ transition is characterized by the Doppler width, while the width of the $3 \rightarrow$ high-$n$ transition is actually dominated by the motional Stark effect. Incidentally, Zeeman effect can be neglected because it mixes the *ortho*- and *para*-Ps states with $m_s = 0$ [18], leading to the well-known enhancement of the average annihilation rate of the Ps ground state (called magnetic quenching) [19] and finally leaving only the unperturbed states $m_s = \pm 1$ in the Ps cloud. By observing that the electric dipole selection rules for optical transitions impose conservation of spin quantum numbers, in first approximation we can assume that the Zeeman effect does not affect the laser excitation process.

The spectral profile of the laser intensity for the first pulse is assumed, for the sake of definiteness, as a Gaussian function whose width at half maximum (FWHM) $\Delta\lambda$ should be matched to the Ps Doppler bandwidth. For the second pulse, the laser intensity spectral profile can be assumed not necessarily Gaussian, but must cover a selected bandwidth of Rydberg sublevels around a reference $n$ state. These broad laser linewidths have a coherence time $\Delta t_{coh} = \lambda^2/c\,\Delta\lambda$, where $\lambda$ is the central wavelength of the proper transition. This parameter turns out to be orders of magnitude shorter than the average duration of laser pulses, around the reference of 5-ns as discussed in the above Section, hence we have to operate with a completely incoherent excitation for both transitions.

The Ps cloud, emerging nearly isotropically from the silica target (see Fig. 1), is assumed thermalized [10,20] with a theoretical Doppler broadening around $4.4 \times 10^{-2}$ nm FWHM for the first transition at the reference temperature of 100 K. However, the Ps atoms which are useful for $\overline{H}$ synthesis by charge exchange reaction, and therefore targets for laser excitation, are only those crossing the antiproton bunch in their fly. The trajectories of this group of atoms lie within the angular cone starting from the generating point and ending at the cigar-like shape antiproton cloud, as in Fig. 1; the line broadening of the first transition relative to these Ps atoms is estimated to be $\Delta\lambda_D = 4.5 \times 10^{-3}$ nm (32 GHz at 205 nm wavelength).

We define the saturation fluence for laser pulse incoherent excitation in the frame of a two-level rate equations model [7], as the fluence which gives 43% of excited population. For the first transition it comes out to be

$$F_{\mathrm{sat}}(1 \rightarrow 3) \simeq \frac{c^2}{B_{1\rightarrow 3}} \sqrt{\frac{2\pi^3}{\ln 2}} \cdot \frac{\Delta\lambda_D}{\lambda_{13}^2} \simeq 11\ \mu\mathrm{J/cm^2} \qquad (1)$$

where $B_{1\rightarrow 3}(\omega)$ is the absorption Einstein coefficient appropriate to the dipole-allowed transition. This equation gives the minimum pulse fluence needed for reaching saturation of the transition. The energy of the exciting laser pulse will depend on the laser spot-size, which must overlap the Ps cloud. The transverse pulse FWHM dimension of the laser, assuming a Gaussian profile for simplicity, is requested to be $\Phi = 3$ mm (according to the Ps cloud cross-section of 6 mm$^2$ of AEGIS proposal). In order to cover the whole FWHM of the cloud with a fluence higher or at least equal to the saturation value $F_{sat}$, the fluence $F_0$ at the intensity maximum is fixed to $F_0 = 2F_{sat}$; the laser pulse energy ($E = \pi(F_0/2)(\Phi/1.177)^2$ for a Gaussian transverse profile) then comes out to be $E_{13} = 2.2\mu$J.

In relation to the second transition $n = 3 \rightarrow$ high-$n$, the motional Stark effect on Ps atoms at 100 K temperature and 1 T magnetic field leads to the opening and mixing up of the originally near degenerate $l, m$ sublevels belonging to a definite $n$ and, moreover, to an interleaving of different sublevel manifolds for $n$ higher than 16. The broadening of the sublevel structure, which can be considered as a quasi-continuum due to their huge number (a Rydberg level band), can be as high as 10 nm ($\sim$1 THz), overwhelming larger

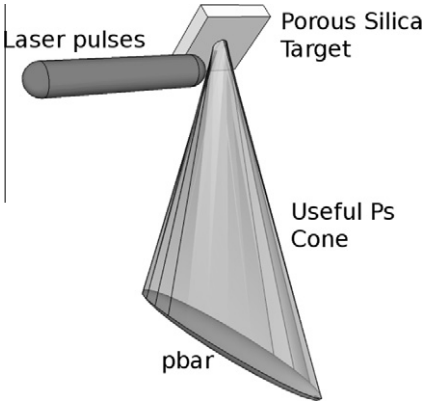


**Fig. 1.** Sketch of the Ps atoms generation, excitation and overlapping with the $\bar{p}$ cloud. Only the Ps atoms flying in the angular cone impinging the cigar-like shape $\bar{p}$ cloud are useful for $\overline{H}$ generation.

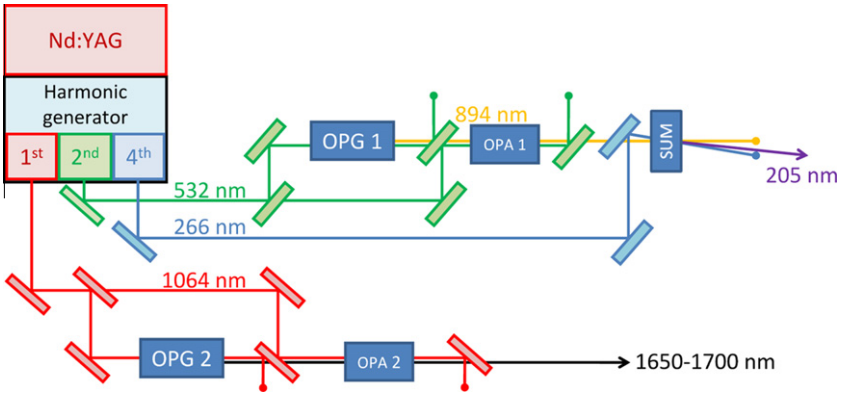


**Fig. 2.** Laser system for the Rydberg excitation of Ps.

than the Doppler broadening of 0.4 nm. In the full mixing range $n > 16$ [18], the saturation fluence for the second transition results largely independent of $n$ and of the laser linewidth and comes out to be

$$F_{\mathrm{sat}}(3 \to n) \simeq \frac{c \times 13.6\ \mathrm{eV}}{B_{3\to n}\hbar n^3} \simeq 0.98\ \mathrm{mJ/cm^2} \qquad (2)$$

for the reference $n = 25$. The linewidth of the laser pulse can be chosen in the range of 1–4 nm, greater than the Doppler broadening and limited by the requirement of exciting a number of final $n$ states sufficiently low. The total energy of the laser pulse required for saturating this Rydberg level, using the same cloud parameters of the previous transition, results in $E_{3n} = 174$ μJ.

A numerical simulation of excitation processes with the above laser fluence and energy, and taking care of losses due to spontaneous emission and photo-ionization, gives an excitation probability of about 30% of Ps atoms in the selected Rydberg state, slightly less than the theoretical efficiency limit of 33% for a simultaneous three-level two-step incoherent excitation [7]. For comparison, a parallel calculation performed by exploiting the alternative excitation path $1 \to 2 \to$ high-$n$ gives a fraction of excited Ps of 24%, well below the previous and supporting the discussion about the choice between the possible excitation sequences.

## 3. The proposed scheme of the laser system for Ps excitation

The wavelengths of the two lasers are, respectively, $\lambda = 205$ nm for the excitation from ground to $n = 3$ state, and $\lambda$ in the range [1650−1700] nm for the in-cascade transition. The two lasers have to generate the wide spectral bandwidth matching the quasi-continuum level bandwidths of the two Ps transitions. Moreover, the final goal of the maximum excitation Ps efficiency must be reached with the minimal possible energy per pulse, due to the constraint of the minimal energy dispersion in the cryogenic interaction chamber of AEGIS. The required pulse bandwidths are so wide, especially that for the second transition, that standard lasers based on optical cavities embodying the laser material are not suited for our Ps excitation. In fact, these lasers operate at definite longitudinal modes giving a relatively narrow width lines inside the spectrum envelope. This imply a notable reduction of excitation efficiency with respect to laser pulses with continuous spectrum operating with the same total energy, because the total width of the Ps resonance is not covered and therefore not saturated by the comb-like shape of the spectrum.

The laser technology developed to produce a wide continuum spectrum necessary for efficient excitation, an essential goal in our case, is that based on the optical parametric generation and amplification [21].

We consider the laser system schematized in Fig. 2. Both radiations are generated through second-order polarization in optical crystals. The 205 nm radiation is obtained by summing up in a non-linear BBO crystal the 266 nm fourth-harmonic of the 1064 nm Nd:YAG radiation and the 894 nm radiation generated in an OPG (Optical Parametric Generator). This radiation is produced by means of a down conversion process from the 532 nm second-harmonic of the Nd:YAG, and further amplified with an OPA (Optical Parametric Amplifier), in order to fulfill the requirements about the acceptance region of the BBO crystal for greater energy production. The other wavelength is generated more directly in a single step by an OPG, and then amplified by an OPA.

In this layout a Q-switched Nd:YAG laser delivering a maximum of 650 mJ in 4 − −6 ns drives both laser systems. About half the energy of the Nd:YAG laser is conveyed along the first system (the upper part of Fig. 2), where it is frequency doubled to the 532 nm second harmonic for pumping the OPG1, the OPA1 and a second frequency doubling crystal producing the 266 nm radiation. The remainder of the 1064 nm radiation pumps both the OPG2 (a small fraction) and the OPA2.

The proposed laser system provides spectral bandwidths large enough to cover the Ps level broadenings as well as the power levels to meet the requirements as discussed in Section 2. The laser of the second transition has in addition the capability to operate at frequencies within ∼30 nm around the 1670 nm. This allows the selection of the final Ps excited energy (starting from $n = 16$ up to the ionization limit) and gives margin for possible unexpected problems in the excitation. The pulse duration cannot exceed a few nanoseconds in order to be consistent with the Ps flight time from the silica slab to the $\bar{p}$ cloud and, moreover, to minimize losses due to enhanced annihilation after spontaneous decay to the ground state due to sublevel magnetic mixing.

The pulse energies and spectral bandwidth can satisfy the requirements for maximization of the Ps transition efficiency. We have the goal of generating pulses with an energy up to ten times higher than the energy estimated by saturation fluence calculations, for having a large safety margin on the amount of energy at disposal. In fact, (i) the excitation calculation is made assuming a simplified model [7,18], (ii) the losses of the pulse transport line can be at the moment only assessed being the transport line very critical and (iii) the Ps cloud formation and flight and, in addition, the atom temperature are only hypothesized. With this system layout the energy goal seems to be reasonably confident.

## 4. The design and test of the laser system for the second transition

We first describe in detail the more simple design of the laser system part devoted to the production of the infrared radiation,

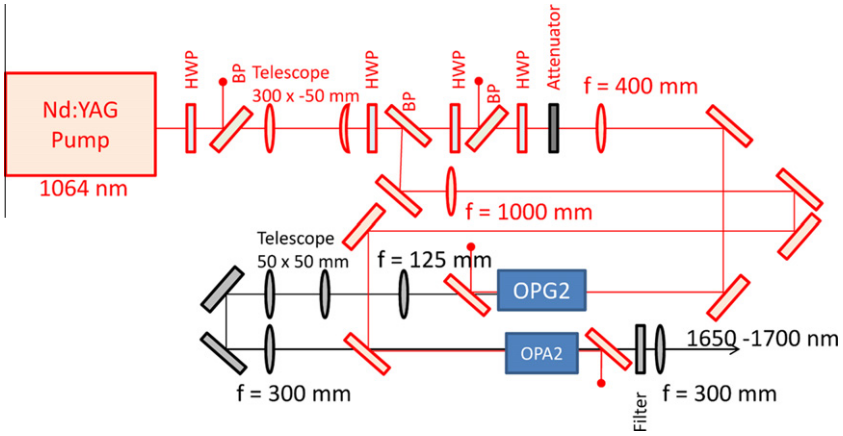


**Fig. 3.** Experimental schematic: HWP, half-wave plate; BP, Brewster plate.

and present the results of the relative tests. In our experiment both the wavelength and the linewidth of the radiation of this second laser pulse are not fixed in advance, therefore the laser system must have wavelength tunability with the required pulse energy and bandwidth. The OPG2-OPA2 source has to provide a radiation pulse with the following characteristics: tunable wavelength in the range $\lambda = 1650-1700$ nm, pulse length $\tau < 10$ ns, pulse energy up to 2 mJ and a quasi-continuous spectrum with a linewidth $\Delta\lambda$ up to 4 nm, covering a Rydberg level band wide section. These requirements cannot be satisfied simultaneously by commercial laser sources. The optical layout assembled in our Lab is shown in Fig. 3.

In the test we have used a Q-switched Nd:YAG laser providing pulses of 150 mJ, $\sim 5$ ns FWHM long, with a repetition rate of 2 Hz. The beam profile is almost circular with $M^2 = 1.4$.

The OPG2 consists of a commercially available Periodically Poled Potassium Titanil Phosphate (PPKTP) [22] crystal with a periodicity of 37.4 μm; for different frequency generation intervals another periodicity can be used. The crystal is 40 mm long and has a $1 \times 2$ mm$^2$ transverse section. It has a very high non-linear coefficient [23] ($d_{eff} \simeq 9$ pm/V) and operates in the Quasi-Phase Matching (QPM) condition [24] converting a 1064 nm photon in two photons: a *signal* photon with $\lambda \in [1600, 1700]$ nm and an *idler* photon with $\lambda \in [2600, 3000]$ nm. In this kind of noncritical down-conversion process the required wavelength flexibility on *idler* and *signal* is obtained by controlling the crystal temperature [21]. A small fraction of the Nd:YAG laser total power is conveyed into the OPG2 crystal by a system of a half-wave plate together with a polarizing Brewster-window. Within the PPKTP crystal the pump beam has a waist of 400 μm FWHM. The wavelength emission is finely tuned by a temperature-controlled heater and it is operated between room temperature and 130 °C. The wavelength range as function of the temperature is shown in Fig. 4. The input–output energy graph is shown in Fig. 5. Using an input pump energy of about 2 mJ (corresponding to $\sim 80\%$ of the crystal damage threshold) we can obtain up to 200 μJ at 1670 nm. The pulse from PPKTP has a spectrum of 2 nm. The output of the OPG2 beam is collimated with a 125-mm focal length lens. The energy jitter for the crystal is about 2 μJ.

We remark that the pump comb-like spectral profile (due to the laser operation on the cavity modes) is transformed by the down-conversion process into an almost continuous spectrum peaked at the chosen wavelength. This occurs because the much wider contributions from the various frequency components of the pump sum up incoherently.

The parametric amplification of the OPG2 radiation pulse is achieved with an OPA system based on a pair of KTP crystals 10 mm long and $5 \times 5$ mm$^2$ cross-section. This device transforms Nd:YAG pump photons into signal photons by a stimulated

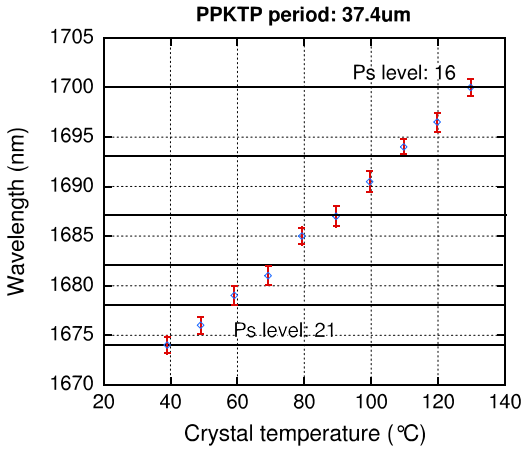


**Fig. 4.** Graph of the wavelength output as function of the temperature for the PPKTP crystal. The horizontal full lines correspond to the wavelengths for excitation of the indicated Ps $n-$levels.

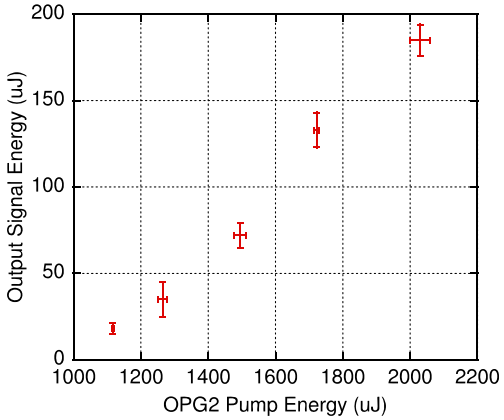


**Fig. 5.** Graph of OPG2 energy output as function of the pump energy.

down-conversion process. The amplified output can reach 3 mJ at 1670 nm with an input pulse of 100 μJ from the PPKTP.

The 1670 nm radiation coming from OPG2 is selected among other wavelengths by a dichroic mirror and a filter highly transmissive for wavelengths longer than 720 nm. This seed is focused on the OPA crystal with a 550 μm waist FWHM, superimposed to a 750 μm FWHM pump pulse in a type II phase matching scheme.

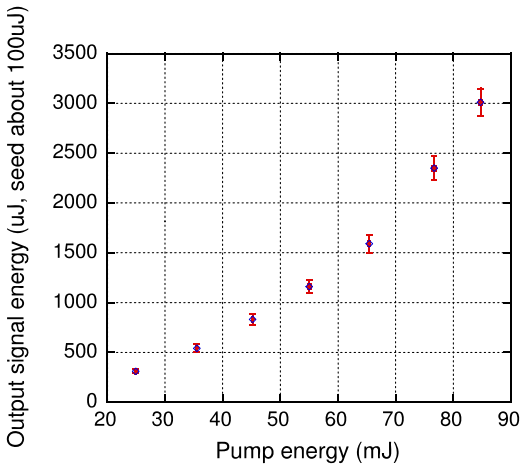


**Fig. 6.** Graph of energy output as function of the pump energy on OPA2.

OPA2 performance was investigated as function of the pump energy. Attention had to be paid, in operation above threshold, to pump energy and alignment to avoid emission of broadband unseeded OPG from the second stage. In Fig. 6 the output energy versus the input energy is shown.

We remark that the point-to-point (natural) instability (~50 μrad) of the pump constrained to compact the OPG design as much as possible, willing to minimize the jittering in the signal-pump overlap, in order to minimize the output energy-jitter. A further contribution to the observed jitter is due to the waist dimension jitter of the pump beam.

In conclusion we can obtain a maximum of about 3 mJ, many times the saturation energy, so we can operate with a safety margin useful for unseen future problems as discussed in Section 3.

## 5. The design and test of the laser system for the first transition

Summarizing the discussion presented in Sections 2 and 3, on the laser system at 205 nm responsible for the excitation ($n = 1 \rightarrow n = 3$) we have the following requirements:

1. spectral bandwidth larger than 30 GHz RMS, mainly accounting for the Doppler broadening,
2. an almost continuous spectrum (*i.e.* without the comb-like structure typically due to the mode spacing of an optical cavity),
3. a pulse duration shorter than 10 ns,
4. an integrated energy many times larger than 2.2 μJ.

The requirements on the spectral properties and the pulse duration are easily fulfilled by using an optical parametric converter (OPG1) pumped by a Q-switched pump laser and amplified in a bulk crystal (OPA1). Hence this approach is in fact preferred over others schemes, like tripling of 615 nm suggested in [6] and proposed in a former Ps excitation scheme [3]. On the other hand the requirements on the wavelength and the energy per pulse are not as trivial to be fulfilled. In fact producing 205 nm photons by direct parametric down-conversion is not realistic because of the lack of suitable pump lasers at wavelengths shorter than 205 nm. Alternative approaches based on harmonic generation, such as frequency doubling or tripling, on down-converted photons at longer wavelength are not viable mainly because of the limited efficiency reachable in the harmonic process.

Given these constraints, we have considered a different approach based both on parametric down-conversion and frequency summing processes [26,27]. Here the requirements (1) and (2) are satisfied by generating radiation at 894 nm with an OPG pumped by a nanosecond laser at 532 nm. Subsequently the 894 nm light is frequency summed to the second harmonic of the same pump laser, at a wavelength of 266 nm, finally generating 205 nm radiation. Compared to the case of direct harmonic generation of the OPG radiation, with our approach the conversion process towards 205 nm is considerably more effective because of the large amount of energy available at 266 nm with nanosecond lasers which boosts the nonlinear conversion towards the deep UV. From the spectral point of view the frequency summing process consist in adding the continuous spectrum from the OPG to the comb-like spectrum of the 266 nm radiation (obtained as the fourth harmonic of a Q-switched Nd:YAG lasers), hence resulting in the required continuous spectrum peaked at 205 nm.

A sketch of the experimental layout for the test of this laser system is depicted in Fig. 7. The pump is a 6-ns pulsed Nd:YAG doubled to 532 nm, giving an energy about 75 mJ per pulse. A beam splitter sends a small part of the 532 nm pulse to the OPG1 generating 894 nm radiation. The remainder is used for pumping the OPA1 crystal after traversing a second frequency doubling stage, based on a BBO nonlinear crystal, which can convert up to 13 mJ of the energy into a 266 nm pulse.

The OPG1 is based on a 30 mm long Periodically Poled KTP crystal (PPKTP) with transverse dimensions $1 \times 2$ mm$^2$. The crystal is pumped with pulses up to 3 mJ, resulting in pulses of energy up to 500 μJ in the infrared [27]. Because the measured spectrum of these pulses increases with the pump power, resulting in a bandwidth that can be so broad as several nanometer, we choose to operate in a range less than half of the maximum power in order to have a controlled narrower spectrum of about 3 nm. A plot of the 894 nm radiation energy produced is shown in Fig. 8, as a function of the pump energy. In order to have more energy on the spectral acceptance band of the sum frequency crystal (that is about 100 GHz, or 0.3 nm) we used an OPA composed by two 12-mm long BBO crystals (OPA1 in Fig. 7) in a type-I phase matching condition, pumped by the 532 nm pulse not converted to 266 nm. Both the green pump and the infrared signal have a FWHM dimension of

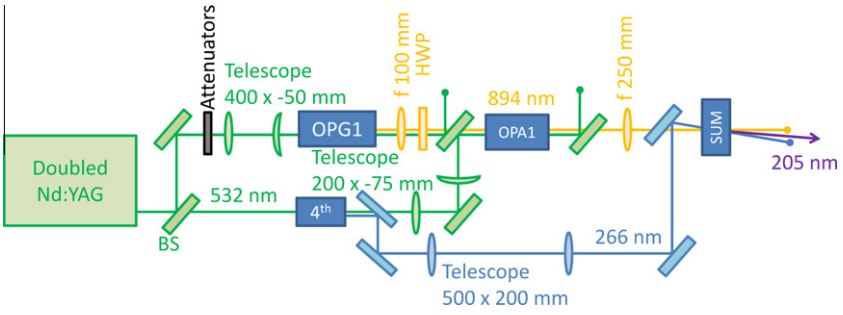


**Fig. 7.** Scheme of the laser system for 205 nm generation. HWP: half-wave plate; BS, beam splitter.

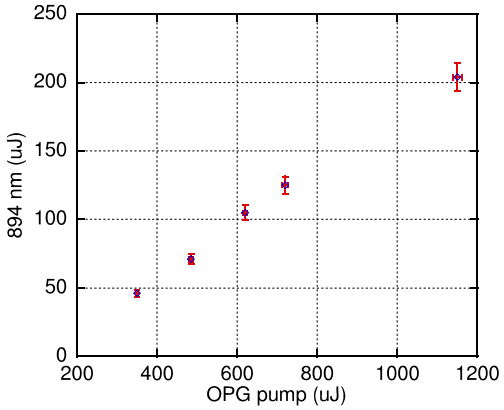


**Fig. 8.** Graph of the energy produced by OPG1 as a function of the pump energy.

1.7 mm. This amplification stage can rise the signal energy up to 7 mJ, as shown in Fig. 9 for two sets of experimental data corresponding to different OPG1 signal energies. It is apparent from the figure that the OPA1 gain is lower for higher OPG1 signal energies; this because the acceptance band of the two crystal system (600 GHz, 1.6 nm) selects only a part of the OPG1 signal bandwidth for the amplification.

As described before, the OPA1 is pumped with the non-converted green beam exiting out from the fourth harmonic BBO crystal. The maximum output in amplification was obtained by using all the available 532 nm pump energy not used in the OPG1 stage, by means of a suitable tilting of the former crystal out of phase matching. In order to reach the final goal of maximizing the 205 nm radiation, we have to align this crystal pursuing the best phase matching condition for 266 nm generation; hence the 532 pump energy is reduced by the quantity converted to this wavelength. The amplified signal energy at 894 nm in this optimized operative condition is within 3 and 4 mJ, as shown in the right part of Fig. 10.

Finally, the frequency summing stage is composed by a dichroic mirror superposing the radiations at 894 and 266 nm, followed by a BBO crystal (labeled SUM in Fig. 7) cut to satisfy the type-I phase matching condition for the process 894 nm + 266 nm → 205 nm, and 5 mm long in order to insure a large nonlinear conversion bandwidth. The two pulses cross the crystal in a noncollinear configuration, with an angle of 5° between the 894 nm pulse and the 266 nm pulse, in order to separate the 205 nm from the more intense 266 nm: the 205 nm pulse forms an angle of 1°9′ with the former. Both pulses have a FWHM transverse dimension of 2 mm.

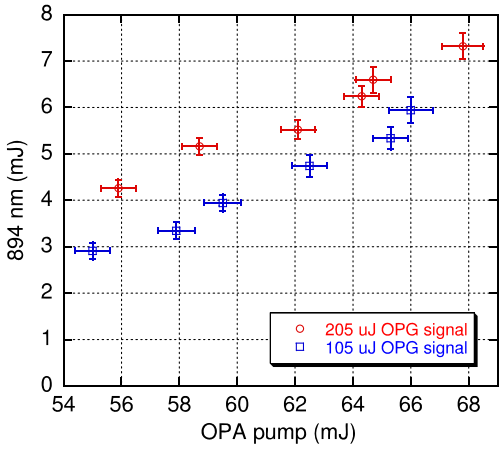


**Fig. 9.** Graph of the energy produced by OPA1 as a function of the pump energy, starting from two different signal inputs as indicated.

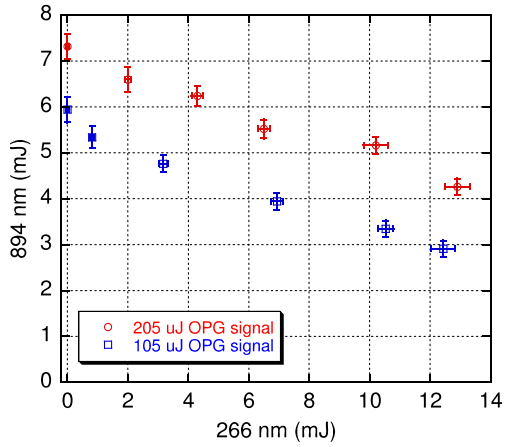


**Fig. 10.** Plot of energy pulse produced by OPA1 correlated with the energy of 266 nm pulse for the layout of Fig. 7. The experimental data are obtained by varying the phase matching condition of the fourth harmonic crystal.

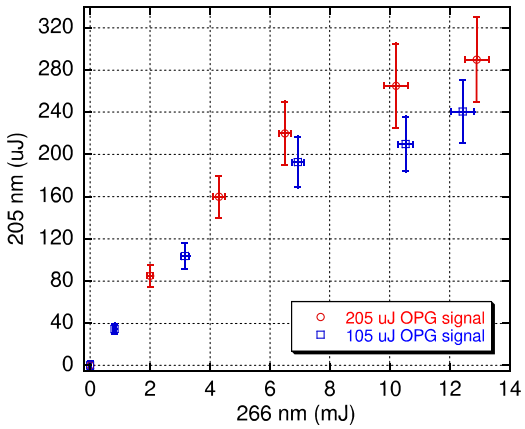


**Fig. 11.** Graph of the 205 nm energy produced by the sum crystal, as function of the fourth harmonic energy.

As shown in Fig. 11, we obtain about 240 μJ at 205 nm for the first set of experimental data and 300 μJ for the second set. In both cases, the energy is well over the saturation energy of 2.2 μJ required on Ps after traversing the transfer line into the experimental chamber, hence with a large safety factor preventing the contingency of high losses in transfer line.

## 6. Conclusions

In this paper we have proposed and demonstrated a new laser system tailored to the task of efficient excitation to Rydberg levels of Ps atoms immersed in a magnetic field, an intermediate step required by the AEGIS experimental proposal for which the synthesis of a large number of antihydrogen atoms is pursued. The system consists of two coupled lasers, one addressed to the $1 \rightarrow 3$ and the other to the $3 \rightarrow n$ transition. Both lasers are essentially based on the technology of parametric generation and amplification, which was chosen because it is appropriate for laser sources with large frequency bandwidth and near continuous spectrum. The laser systems have enough power to guarantee a 30% transition efficiency. The built and tested system can cover a frequency band wide enough to excite different Rydberg levels maintaining a great flexibility for the choice of the best strategy for obtaining a large number of antihydrogen atoms.

## Acknowledgment

We acknowledge the technical support by D. Cipriani.

## References

[1] A. Kellerbauer, AEGIS collaboration, et al., Nucl. Instr. Meth. B 266 (2008) 351.
[2] Available from: <http://doc.cern.ch/archive/electronic/cern/preprints/spsc/public/spsc-2007-017.pdf>.
[3] M.G. Giammarchi, AEGIS collaboration, et al., Hyperfine Interact. 193 (2009) 321.
[4] E.A. Hessels, D.M. Homan, M.J. Cavagnero, Phys. Rev. A 57 (1998) 1668.
[5] A. Speck, C.H. Storry, E.A. Hessels, G. Gabrielse, Phys. Lett. B 597 (2004) 257.
[6] C.H. Storry et al., Phys. Rev. Lett. 93 (2004) 263401.
[7] F. Castelli, I. Boscolo, S. Cialdi, M.G. Giammarchi, D. Comparat, Phys. Rev. A 78 (2008) 052512.
[8] D.W. Gidley, H.G. Peng, R.S. Vallery, Annu. Rev. Mater. Res. 36 (2006) 49.
[9] R. Ferragut et al., J. Phys.: Conf. Ser. 225 (2010) 012007.
[10] (a) S. Mariazzi, A. Salemi, R.S. Brusa, Phys. Rev. B 78 (2008) 085428; (b) S. Mariazzi, P. Bettotti, R.S. Brusa, Phys. Rev. Lett 104 (2010) 243401; (c) S. Mariazzi, P. Bettotti, S. Larcheri, L. Toniutti, R.S. Brusa, Phys. Rev. B 81 (2010) 235418.
[11] S.M. Curry, Phys. Rev. A 7 (1973) 447.
[12] C.D. Dermer, J.C. Weisheit, Phys. Rev. A 40 (1989) 5526.
[13] S. Chu, A.P. Mills Jr., Phys. Rev. Lett. 48 (1982) 1333.
[14] K.P. Ziock, C.D. Dermer, R.H. Howell, F. Magnotta, K.M. Jones, J. Phys. B: At. Mol. Opt. Phys. 23 (1990) 329.
[15] K.P. Ziock, R.H. Howell, F. Magnotta, R.A. Failor, K.M. Jones, Phys. Rev. Lett. 64 (1990) 2366.
[16] B.W. Shore, K. Bergmann, A. Kuhn, S. Schiemann, J. Oreg, J.H. Eberly, Phys. Rev. A 45 (1992) 5297.
[17] B. Broers, H.B. van Linden van den Heuvell, L.D. Noordam, Phys. Rev. Lett. 69 (1992) 2062.
[18] F. Castelli, M.G. Giammarchi, in: Proceedings of the International School of Physics "Enrico Fermi", Course CLXXIV: Physics with many Positrons, IOS press Amsterdam, 2010.
[19] A. Rich, Rev. Mod. Phys. 53 (1981) 127. and references therein.
[20] D.B. Cassidy, P. Crivelli, T.H. Hisakado, L. Liszkay, V.E. Meligne, P. Perez, H.W.K. Tom, A.P. Mills Jr., Phys. Rev. A 81 (2010) 012715.
[21] R.W. Boyd, Nonlinear Optics, third ed., Academic Press, 2008.
[22] S. Haidar, T. Usami, H. Ito, Appl. Opt. 41 (2002) 5656.
[23] L.E. Myers, G.D. Miller, R.C. Eckardt, M.M. Fejer, R.L. Byer, W.R. Bosenberg, Opt. Lett. 20 (1995) 52.
[24] M.M. Fejer, G.A. Magel, D.H. Jundt, R.L. Byer, IEEE J. Quantum Elect. 28 (1992) 2631.
[26] A. Borsutzky, R. Brunger, R. Wallenstein, Appl. Phys. B 52 (1991) 380.
[27] M. Becucci, G. Ferrari, I. Boscolo, F. Castelli, S. Cialdi, F. Villa, M.G. Giammarchi, J. Mol. Struct., in press, doi:10.1016/j.molstruc.2011.01.064.